Soft Matter

Dependence of Adhesive Friction on Surface Roughness and Elastic Modulus

Journal:	*Soft Matter*
Manuscript ID	SM-ART-02-2022-000163.R1
Article Type:	Paper
Date Submitted by the Author:	23-May-2022
Complete List of Authors:	Maksuta, Daniel; University of Akron, Polymer Science Dalvi, Siddhesh; University of Akron, Polymer Science Gujrati, Abhijeet; University of Pittsburgh Pastewka, Lars; University of Freiburg, Microsystems Engineering Jacobs, Tevis; University of Pittsburgh, Mechanical Engineering & Materials Science Dhinojwala, Ali; University of Akron, Polymer Science

Dependence of Adhesive Friction on Surface Roughness and Elastic Modulus

Received 00th January 20xx,
Accepted 00th January 20xx

DOI: 10.1039/x0xx00000x

Daniel Maksuta,[a†] Siddhesh Dalvi,[b†] Abhijeet Gujrati,[c] Lars Pastewka,[d] Tevis DB Jacobs,[c] Ali Dhinojwala *[b]

Friction is one of the leading causes of energy loss in moving parts, and understanding how roughness affects friction is of utmost importance. From creating surfaces with high friction to prevent slip and movement, to creating surfaces with low friction to minimize energy loss, roughness plays a key role. By measuring shear stresses of crosslinked elastomers on three rough surfaces of similar surface chemistry across nearly six decades of sliding velocity, we demonstrate the dominant role of adhesive frictional dissipation. Furthermore, while it was previously known that roughness-induced oscillations affected the *viscoelastic* dissipation, we show that these oscillations also control the molecular detachment process and the resulting *adhesive* dissipation. This contrasts with typical models of friction, where only the amount of contact area and the strength of interfacial bonding govern the adhesive dissipation. Finally, we show that all the data can be collapsed onto a universal curve when the shear stress is scaled by the square root of elastic modulus and the velocity is scaled by a critical velocity at which the system exhibits macroscopic buckling instabilities. Taken together, these results suggest a design principle broadly applicable to frictional systems ranging from tires to soft robotics.

Introduction

Friction plays an important role in natural and engineering processes from a tire gripping the road,[1] to the sliding of a human finger on a haptic screen,[2] to a robotic gripper picking up an object,[3] to a lizard running up a vertical wall.[4,5] The biggest barrier to improving performance in these areas is a fundamental-science gap in the understanding of how friction depends on surface roughness.[6-8] For smooth soft adhesive materials this is of particular importance at low sliding velocities where differences in surface properties have been shown to heavily influence the observed friction,[8-12] whereas the presence of frictional instabilities at higher sliding velocities causes friction to become independent of surface properties.[8-16]

In the pre-instability regime, friction is hypothesized to arise from the coupling of adhesive[17-19] and viscoelastic dissipation[20-26] processes. The first dissipative process is often called “adhesive friction” and arises from the adhesion of the interfacial polymer chains, where the energy loss is dictated by the periodic breaking and reforming of the adhesive interactions.[17-19] We note that adhesive friction arises even in cases where there is no measurable macroscopic pull-off force typically associated with “adhesion”, since there are always microscopic attractive interactions.[20,21] The second loss mechanism during sliding is viscoelastic dissipation due to the forced oscillations of the rubber at the interface when conforming to the roughness.[20] Through these oscillations energy is dissipated via heat in proportion to the material’s loss modulus and roughness, resulting in increased friction. Despite the fundamental differences in frictional mechanism, the models for adhesive and viscoelastic friction both predict a similar bell-shaped frictional response as a function of velocity, and it has been difficult to investigate the differences between these two mechanisms.[7,17-19,27-30]

In last two decades, the emphasis has been on describing the viscoelastic contribution to soft-material friction, with only recent advances in understanding the adhesive contribution. For viscoelastic friction, Persson has proposed a quantitative model (without any adjustable parameters) that relates a surface’s roughness, measured over many length scales, to the viscoelastic dissipation during sliding.[19,22,28] For adhesive friction, roughness is only incorporated in a limited way: through changes in the true contact area.[27-29] However, this conceptualization of how roughness influences adhesive friction neglects the possibility that the roughness-induced oscillations—may influence the resulting adhesion.[31] Thus, the fundamental question is: how does surface topography influence the molecular processes governing friction in soft materials?

[a] [a]*Department of Biology, Integrated Bioscience Program, The University of Akron, Akron, Ohio, 44325, United States*
[b] [b]*School of Polymer Science and Polymer Engineering, The University of Akron, Akron, Ohio 44325, United States*
[c] [c]*Department of Mechanical Engineering and Materials Science, University of Pittsburgh, Pittsburgh, Pennsylvania, 15261, United States*
[d] [d]*Department of Microsystems Engineering, University of Freiburg, 79110 Freiburg, Germany.*
†Both contributed equally to this work
*Corresponding author, email: ali4@uakron.edu
Electronic Supplementary Information (ESI) available: [details of any supplementary information available should be included here]. See DOI: 10.1039/x0xx00000x

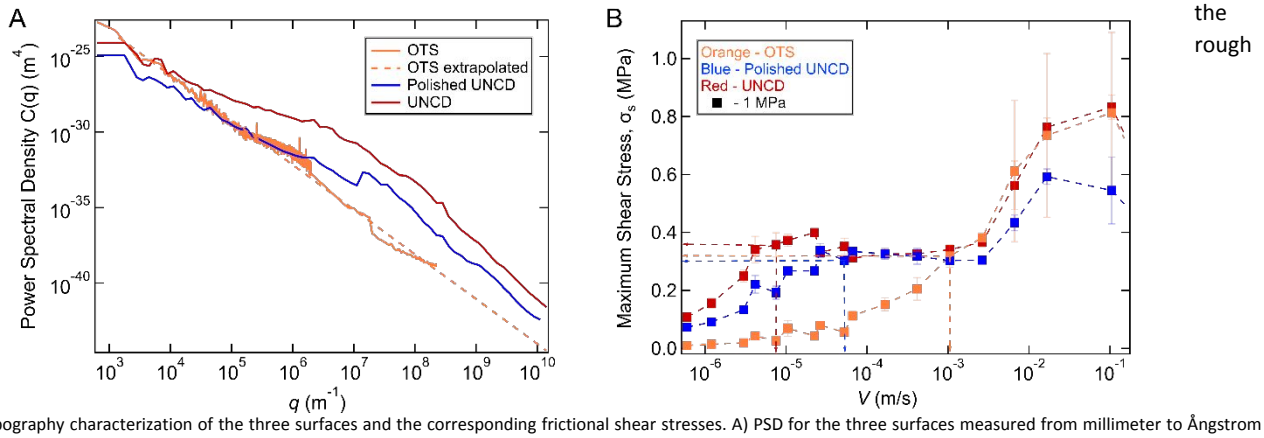

Figure 1. Topography characterization of the three surfaces and the corresponding frictional shear stresses. A) PSD for the three surfaces measured from millimeter to Ångstrom length scales. The value of $C(q)$ (power spectral density) which is proportional to the amplitude of the roughness increases from OTS (purple) to pUNCD (blue) to UNCD (red). We use extrapolation for OTS to estimate the roughness in the nanometer to Ångstrom length scales (dotted purple line). B) Example of experimentally observed frictional shear stress, σ_s, versus sliding velocity, V, for the three surfaces (OTS, pUNCD, and UNCD) with PDMS of 1 MPa modulus. The vertical dashed lines correspond to the onset velocity for Schallamach waves (buckling instability), $V_{SW-onset}$, observed for the different surfaces. One key observation is that friction varies with roughness in the pre-buckling instability phase. We will limit our analysis to the pre-buckling instability regime. Normal force is 5 mN. Error bars correspond to standard deviations calculated from three repeats.

Here, we have designed experiments to answer this fundamental question by disentangling viscoelastic and adhesive contributions to friction, and determining the effects of roughness, modulus, and contact area on adhesive friction. We have conducted *in situ* sliding experiments for highly crosslinked polydimethylsiloxane (PDMS) elastomers with real-time measurements of contact area and cantilever deflection using high-speed video, with variations of almost six decades of sliding velocity and order-of-magnitude variation in elastic modulus. We have chosen three surfaces with similar surface chemistry (non-polar bonds) that vary systematically in surface topography, Ultrananocrystalline diamond (UNCD), polished UNCD and a smooth octadecyltrichlorosilane (OTS) monolayer coated on single-crystal silicon wafer. The methods for preparation of the two rough diamond surfaces are described in detail in refs. [33, 34]. The OTS self-assembled monolayer deposition procedure (described in the methods section) is performed according to ref. [32] to create a molecularly smooth low-energy surface. This ensures that any differences in the observed friction arise primarily due to differences in surface roughness. In this paper we demonstrate the critical importance of adhesive friction in soft materials and propose a model to describe how roughness-induced oscillations modify the interfacial interactions that control friction.

Results and Discussion

The power spectral densities (PSDs) of the three surfaces are shown in **Figure 1a** and the corresponding maximum shear stress σ_s as a function of sliding velocity are shown in **Figure 1b**.[32-34] OTS is the smoothest, followed by polished UNCD, with unpolished UNCD being the roughest. The frictional shear stress during sliding is calculated using deflection and contact area for each frame as obtained from high-speed video of the contact (see Methods). During sliding we observed the emergence of Schallamach waves at a critical onset stress that was independent of surface roughness; however, the onset velocity, $V_{SW-onset}$, decreases with increasing surface roughness. The onset sliding velocity for Schallamach waves was obtained by visual inspection of the high-speed video and is noted with the vertical dashed lines in Figure 1b. Once $V_{SW-onset}$ for the rough surfaces is achieved, a stress plateau regime occurs over two decades of velocity.[8] The end of the plateau regime coincides with the onset of Schallamach waves for OTS. After $V_{SW-onset}$ for smoothest OTS surface, the frictional shear stresses of all surfaces overlap and hence become independent of surface properties.[8] Based on these results, surface roughness only plays a dominant role in the pre-Schallamach wave regime.

Our goal is to disentangle the adhesive and viscoelastic contributions to friction. Specifically, it is commonly understood that $\sigma_s = \sigma_{visc} + \sigma_{adh}$, where σ_s is the frictional shear stress, σ_{visc} is the viscoelastic friction, and σ_{adh} is the adhesive friction. Therefore, we begin by calculating the viscoelastic contribution using Persson's model for friction on rough surfaces. The viscous contribution, σ_{visc}, is attributed to the energy dissipated due to the roughness-induced oscillations occurring at the interface. This model is summarized in four equations below:[22-28]

$$\sigma_{visc} = \int_{q_0}^{q_1} dq q^3 C(q) S(q,V) P(q,V) \int_0^{2\pi} d\phi \cos\phi \frac{E''(qV(t)\cos\phi, T_0)}{(1-\nu^2)} \quad (1)$$

$$S(q,V) = \gamma + (1-\gamma) P(q,V)^2 \quad (2)$$

$$P(q,V) = \mathrm{erf}\left(\frac{1}{2\sqrt{G/\sigma_0}}\right) \quad (3)$$

$$G(q,V) = \frac{1}{8}\int_{q_0}^{q} dq q^3 C(q) \int_0^{2\pi} d\phi \left|\frac{E'(qV(t)\cos\phi, T_0)}{(1-\nu^2)}\right|^2 \quad (4)$$

Here, $E'(qV(t)\cos\phi, T_0)$ and $E''(qV(t)\cos\phi, T_0)$ are the storage and loss modulus respectively evaluated at frequency $qV(t)\cos\phi$ and temperature T_0, ϕ is the orientation of the surface roughness relative to the sliding direction, $S(q,V)$ is a correction factor for the size of the deformation zone, $P(q,V)$ is the ratio of actual contact area to the projected contact area, ν is the Poisson ratio, $\gamma = 1/2$ is a numerical factor (see Ref. [28]), and σ_0 is the normal stress. Since in conformal contact the slope is essentially the strain introduced into the material, Equation 1 can be roughly interpreted as multiplying the squared-strain at scale q with the loss modulus. The model predicts that roughness has two effects on friction: it can modify the magnitude of the observed frictional shear stress; and it can cause a shift in the velocity where friction is maximized. To utilize Equation

1-4 requires denoting the bounds of integration q_0 to q_1, where q_0 is inversely proportional to the contact length and q_1 is inversely proportional to the length scale at which wear processes occur—which is generally determined empirically based on the quality of the fit.[36]

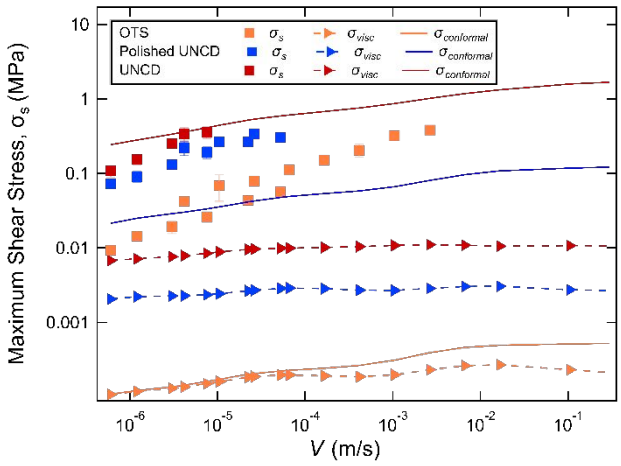

It is also important to note that the conformality predicted using Equation 2-4 neglects adhesive forces.[22-28] While this assumption may be valid for very hard rubbers and or very high sliding velocities, it may not be valid here. Specifically, we have computed the Tabor parameter for our system, assuming 1 to 10 nm asperity radius and surface energy of 40 mJ/m^2. This yields a lower-bound Tabor parameter for the stiffest PDMS of 27 which, together with the low sliding velocity, suggest that these contacts lie in the JKR contact limit where adhesion will be important.[37,38] From this consideration, it is unclear if the calculated conformality is valid; thus, instead we calculate the upper and lower bounds for the viscoelastic friction by assuming either completely conformal contact ($P(q,V) = 1$) or non-adhesive contact, respectively. Where the non-adhesive contact, otherwise known as Hertzian contact, is assumed for Equation 3 and

Figure 2. Log-log plot of the calculated viscoelastic contribution assuming conformal contact (solid lines, $\sigma_{conformal}$) and Hertzian contact (dashed lines with triangles, σ_{visc}) plotted with experimental frictional shear stress data for 1 MPa PDMS plotted against sliding velocity, V, in the pre-instability regime. Experimental data is plotted as square symbols. Calculated viscoelastic contribution does not conform to the trends observed in the experimental data regardless of expected extent of conformality. Storage and loss moduli data comes from Ref. [35]. Error bars correspond to standard deviations calculated from three repeats.

4. **Figure 2** shows the calculated bounds for the viscoelastic contribution using the storage and loss modulus from Ref. [35]. While there is ambiguity in the magnitude of the viscoelastic contribution, ranging from 100 times smaller for the lower bound to comparable for the upper bound, it can be observed that regardless of the conformality the calculated stress for UNCD is greater than pUNCD and OTS across all sliding velocities. Even though the predicted trend of UNCD > pUNCD > OTS matches the experimental results, there are clear quantitative differences between the theoretical predictions and experiment.

Importantly, the prior paragraphs have demonstrated that the magnitude of the measured frictional shear stress cannot be explained by conventional models of viscoelastic friction. This suggests that the dominant mechanism for friction in these materials must be adhesive friction. This result can be explained by the low loss modulus for PDMS, and because adhesive friction is expected to dominate at low sliding velocities.[7,27,28]

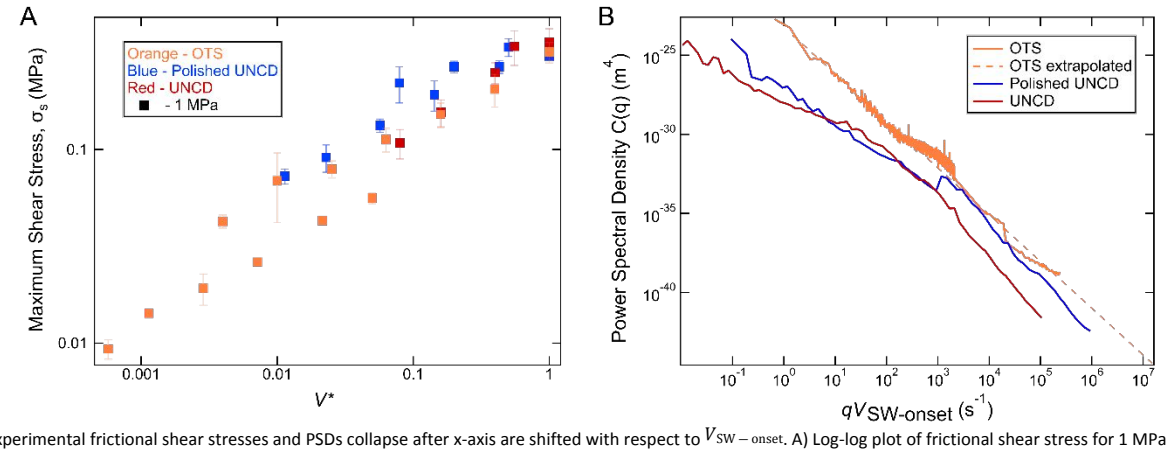

Figure 3. Experimental frictional shear stresses and PSDs collapse after x-axis are shifted with respect to $V_{SW-onset}$. A) Log-log plot of frictional shear stress for 1 MPa PDMS plotted versus $V^* = V/V_{SW-onset}$. B) $C(q)$ plotted versus $qV_{SW-onset}$, where $V_{SW-onset}$ is the onset sliding velocity for Schallamach waves, measured from the high-speed videos. $V_{SW-onset}$ for the various surfaces: $V_{UNCD} = 7.5 \times 10^{-6}$ m/s, $V_{pUNCD} = 6.62 \times 10^{-5}$ m/s, $V_{OTS} = 1.05 \times 10^{-3}$ m/s. Normal force is 5 mN. Error bars correspond to standard deviations calculated from three repeats.

The theory for adhesive friction for smooth surfaces was developed by Schallamach, and later modified by Chernyak and Leonov et al..[17,18] Persson incorporated the influence of roughness in the Schallamach and Chernyak/Leonov model by accounting for regions of non-contact via the pre-factor $P(q_1,V)$ and simplified the velocity dependence by using an exponential function.[27,28] In this theory the adhesive friction has three main factors that influence the magnitude: (1) the strength of the adhesive interactions at the interface; (2) the number of interactions; and (3) the scaling of number of interactions with sliding velocity. The increase in adhesive friction with velocity is related to factor 2, an increase in stretching of the attached chains, which is an entropic effect. After a certain velocity, the number of chains bound to the surface decreases, and this results in a decrease in adhesive friction. This combined effect results in a bell-shape curve represented by Equation 5. The theory postulates that the roughness plays a major role in decreasing friction after the maximum by decreasing the actual contact area or the number of interactions. The equation is

$$\sigma_{\mathrm{adh}} = P(q_1,V)\left\{\tau_{f0}\exp\left(-c\left[\log_{10}\left(\frac{V}{V_0}\right)\right]^2\right)\right\}, \qquad (5)$$

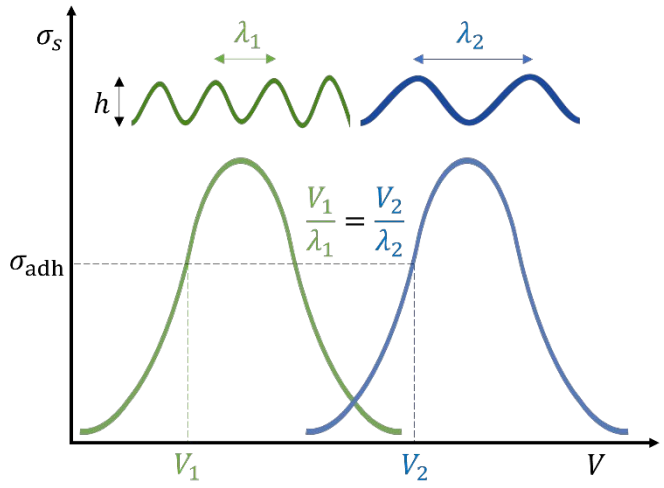

Figure 4. A sketch representing the physical mechanism behind the observed velocity shift of the adhesive contribution to friction. Adhesive shear stress, σ_{adh}, is constant when the oscillation frequency, V/λ (where $\lambda = 2\pi/q$), and magnitude of roughness, h, are equal. The adhesive shear stress is shifted to lower sliding velocities as the wavelength decreases from $\lambda_2$to λ_1. Note that, while similar oscillation-frequency arguments have been previously used to describe viscoelastic friction, these results demonstrate that it also describes adhesive friction.

where τ_{f0} is the interfacial adhesive strength at vanishing sliding velocity, c is a non-dimensional constant related to the rate of increase of frictional shear stress with sliding velocity, V_0 is the velocity at which σ_{adh} is maximum, and $P(q_1,V)$ is the area ratio at length scale q_1. In this equation roughness influences the adhesive response via $P(q_1,V)$, i.e. roughness only influences the amount of contact area. The term in the curly bracket in Equation 5 is a result of stretching of chains attached to the surface, and the parameters τ_{f0}, c and V_0 are expected to be independent of roughness.

We first consider if the differences in friction could be caused by differences in the real contact area between the PDMS and the surfaces. The amount of real contact area is related to both the conformality, via the prefactor $P(q_1,V)$ in Equation 5, and the total amount of surface area available on the surfaces to conform to. First, we consider differences in conformality of the PDMS to the surfaces at V; rather than smaller, OTS should have a larger adhesive stress than pUNCD and UNCD by a factor of 4 and 16, respectively; obviously during experiment we observe the opposite trend of UNCD > pUNCD > OTS. Secondly, if it is due to differences in the amount of available contact area than pUNCD and UNCD should have 1.01 and 1.69 times larger adhesive shear stresses than OTS, respectively.[34] While this difference captures qualitatively the trend, experimentally we observe UNCD and pUNCD a factor of 12 and 8 times greater, respectively, than OTS; therefore, the difference in adhesive friction cannot be explained by differences in contact area alone.

If the differences in magnitude of the adhesive response cannot be explained by differences in surface roughness, then the primary influence of surface roughness on adhesive friction may be to shift the velocity at which the adhesive friction reaches a maximum, i.e. the parameter V_0 that shows up in Equation 5. This hypothesis has a basis in the assumption of the Persson molecular theory, namely that changes in surface roughness can analogously cause a shift in the velocity at which the viscoelastic contribution is maximum.[22-28]

To test the hypothesis that roughness primarily influences V_0, we introduce the dimensionless sliding velocity $V^* = V/V_{\mathrm{SW-onset}}$, where $V_{\mathrm{SW-onset}}$ is the onset velocity for Schallamach waves for the pUNCD, UNCD, and OTS surfaces. Plotting the frictional shear stress versus V^* collapses the data to a master curve (**Figure 3a**), indicating that $V_{\mathrm{SW-onset}}$ takes the role of V_0 in Equation 5. The Schallamach molecular theory assumes that dissipation is driven by periodic excitation of surface chains. For conformal contact, the amplitude of excitation at frequency $\omega = qV_{\mathrm{SW-onset}}V^* \equiv qV$ is related to the PSD $C(q)$. Indeed, plotting the PSD versus $qV_{\mathrm{SW-onset}}$ (**Figure 3b**) collapses pUNCD and UNCD at low frequencies and OTS and pUNCD at high frequencies; this is in reasonable agreement considering that $V_{\mathrm{SW-onset}}$ was estimated visually from high-speed video over a sparsely populated set of V and thus likely carries an uncertainty in addition to the error associated with the PSDs.

Since plotting the frictional shear stress versus V^* produces excellent overlap between the data across variation in roughness, this suggests that there is little difference in the true contact area between the rough surfaces at V^*. When comparing the expected contact area between the surfaces at V^* (instead of V as was done earlier in the text) using Equation 3, we find that the OTS surface should have at least 4 and 15 times more contact area and therefore friction than pUNCD and UNCD respectively. Since we did not observe this difference, it suggests that the presence of adhesion plays a key role in influencing the conformality of the PDMS to the different rough surfaces.[38] However, there is likely a threshold, in terms of both asperity size and elastic modulus, after which the surface forces no longer influence the conformality, as described by the Tabor parameter.[41,42]

These observations suggest that surfaces sliding at the same V^* experience the same excitation spectrum and hence produce the same frictional shear stress—which is summarized in **Figure 4**. The fact that the whole excitation spectrum seems to matter implies that length scales greater than the molecular length scale are important in determining the adhesive frictional response and that the roughness-induced oscillations (qV) play a key role in determining

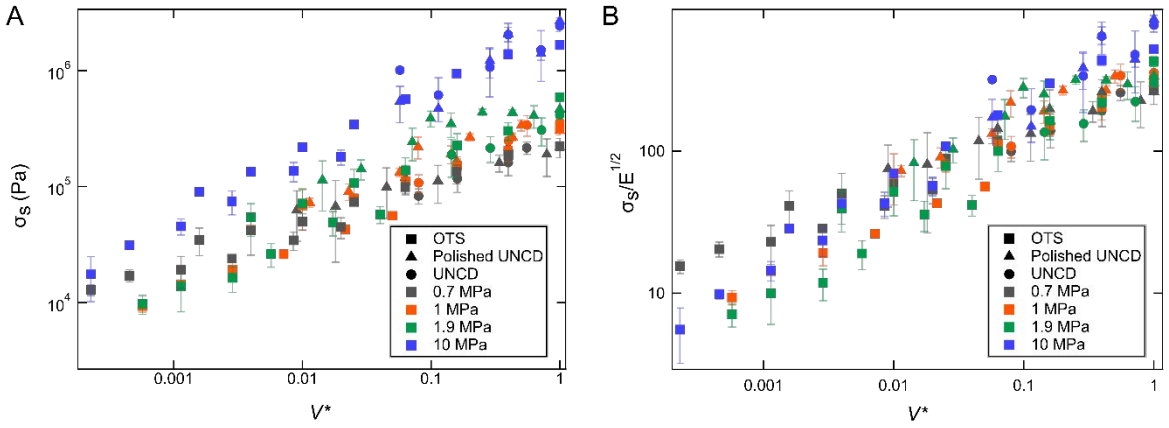

Figure 5. Frictional shear stress as a function of elastic modulus collapses when normalized by elastic modulus raised to the ½ power. A) Log-Log plot of frictional shear stress versus V^* for 0.7, 1, 1.9, and 10 MPa PDMS in the pre-instability regime. Expectation from Equation 5 is that friction should be independent of elastic modulus. B) Log-Log plot of frictional shear stress, σ_s, normalized by the respective elastic modulus raised to the ½ power, plotted against V^* in the pre-instability regime. The overlap of the data after normalization suggests the pre-factor to the adhesive contribution, which is a product of the magnitude and number of interactions, should scale as $\sqrt{\mathrm{N/m^2}}$. Normal force is $5\ \mathrm{mN}$. Error bars correspond to standard deviations calculated from three repeats.

the velocity dependence of both the adhesive and viscoelastic contributions of friction.[17-19,27,28] This is in clear contrast to previous expectations where the adhesive contribution's velocity response was assumed to be only dependent on the chemical identity of the material.[8,18,28] This result also finds analogy with the emergence of surface defects during extrusion where the onset velocity for surface defects is shifted to higher extrusion rates when the exit die is made smoother or of a lesser surface energy.[42]

We would like to add that Müser and Persson recently pointed out that there is another dissipation mechanism they found that leads to a $\sqrt{V}$ velocity dependence, similar to what we observe (see Figure 5).[40] They studied pull-off rather than sliding, but the underlying mechanism should be transferable since the main difference is that the former involves the propagation of a mode I and the latter a mode II/III crack at the contact line. Müser and Persson invoke an argument originally due to Persson and Brener: the high strain at the crack tip leads to a high strain rate during crack propagation and hence a high energy dissipation, albeit localized to the near-field of the crack tip.[41] Integration over the contact line then leads to an overall non-negligible energy dissipation rate. We note that while this theory is qualitatively compatible with our sliding data, we do not observe a strong dependence on rate in pull-off experiments (see ref. [34]) which this model also predicts. We can, however, not rule out that this mechanism may be the dominate source of energy dissipation in other sliding scenarios.

Finally, we measured the effect on friction with variation in elastic modulus of the PDMS. We find, as expected, that frictional shear stress increases with elastic modulus. [18,19,42] Further, it can be observed in **Figure 5a** that the velocity shift of the adhesive contribution is largely independent of elastic modulus—where $V_{\mathrm{SW-onset}}$ occurs at two adjacent sliding velocities across the range of elastic moduli. Additionally, the quality of the overlap of the frictional shear stress within an elastic modulus is independent of elastic modulus. Thus, suggesting that conformality within an elastic modulus is similar across surface roughness.

Next, we consider if the frictional shear stress scales as expected with elastic modulus, which would further support the assertion that conformality is not influenced by surface roughness for systems that are dominated by adhesive friction. Given past results on smooth surfaces we would expect the frictional shear stress to increase with $E'^{1/2}$ to $E'^{3/4}$—i.e. factor τ_{f0} in Equation 5.[19] Indeed, we find that the optimal normalization factor occurs between $E'^{1/2}$ to $E'^{3/4}$ (R^2 values versus normalization factor is shown in **Figure S1**), where results with normalization factor of $E'^{1/2}$ are shown in **Figure 5b**. This result supports the assertion that rather than changes in conformality, surface roughness primarily changes the sliding velocity at which friction is maximum within and across elastic modulus.

This result is unexpected given Equation 3-5; where we would expect the amount of conformality to decrease as E'^{-1} to $E'^{-0.7}$—assuming the loss tangent is independent of elastic modulus—for flat punch (**Figure S2**) and hemispherical, respectively thus causing a deviation from the observed $E'^{1/2}$ scaling. Based on these results it is quite clear that the absence of surface forces in Equation 3-5 leads to incorrect predictions for the friction in adhesive materials; thus, future theoretical work is needed to determine the impact of adhesion on $P(q_1,V)$, or conformality, in addition to roughness, modulus, and velocity.[42] Accurate predictions of $P(q_1,V)$ will provide a more complete understanding of friction in the smooth-sliding regime for soft elastomers on rough surfaces.

Conclusions

For PDMS of various elastic moduli sliding on three rough surfaces with similar interfacial chemistry, we find that interfacial roughness plays a key role in influencing the friction behavior in the pre-buckling-instability regime. The friction is demonstrated to be dominated by adhesive dissipation rather than viscoelastic dissipation. Furthermore, our results reveal two main factors that quantitatively explain the influence of roughness and modulus on adhesive friction. First, contrary to expectations that roughness only influences the available contact area for adhesive friction,[17-19] we find that the roughness-induced oscillations cause a shift in the velocity at which the adhesive friction is maximum. Thus, our results reveal a previously unknown design parameter to control friction in

the pre-instability regime. Second, because the frictional shear stress scales with $E'^{1/2}$, which is expected for adhesive friction on smooth surfaces, this further supports the assertion that roughness primarily influences the velocity at which friction is maximum rather than the conformality of the soft elastomer to the surface. Overall, this investigation provides the critical data to elucidate the behavior of adhesive friction, and its dependence on the roughness and stiffness of the materials.

Methods

The smooth OTS monolayer was deposited on a silicon wafer using a wet chemical deposition method.[32, 44] Smooth silicon wafers (obtained from Silicon Inc.) were cleaned and etched with Piranha solution, washed with ample amount of deionized water and blow dried with nitrogen. After drying, the wafers were air plasma treated in a Harrick Inc. plasma chamber for 5 mins and dipped in a vial containing 1 wt.% solution of Octadecyltrichlorosilane (OTS) (obtained from Gelest Inc.) in toluene for 8 hours, while purging the vial using nitrogen through a septum. The wafers are then rinsed with solvent cycles of different polarity, blow dried and heated in vacuum at 120˚C for 12 hours.

Highly crosslinked PDMS networks were created using a 3-part system from Gelest Inc. that includes the base as vinyl terminated chains of PDMS with a narrow molecular weight distribution (V-05:800 gm/mol, V-21:9,000 gm/mol, V31:28,000 gm/mol, V41:62,700 gm/mol), tetrakisdimethylsiloxysilane (SIT 7278.0) as crosslinker, and platinum carbonyl complex (SIP 6929.2) as catalyst.[19,34,45] We used the vinyl to hydride ratio of 4.4 to avoid formation of side chains and compensate for the loss of crosslinker by evaporation during the curing process. We added 0.1 wt. % catalyst and then gently stirred and use vacuum for about 5 mins to remove air pockets. In case of V-05, the crosslinking reaction accelerates faster because of higher number of reactive groups, thus an inhibitor molecule 1,3,5,7-tetravinyl-1,3,5,7-tetramethyl cyclotetrasiloxane was used to slow down the reaction rate. The detailed procedure of casting and extracting unreacted oligomers from the PDMS lenses using this procedure is described in ref. [34]. The radius of curvature of these lenses were 1.25 mm. The roughness of the PDMS lenses synthesized by the above method (0.5 nm or less) were measured using atomic force microscopy and these values of RMS roughness were much smaller than the roughness of the diamond surfaces and can be considered to be atomically smooth.[46] PDMS lenses synthesized with similar techniques have also reported surface roughness in the range we report.[47] The modulus of the PDMS is characterized by JKR techniques by solving for the elastic modulus and work of adhesion as unknown variables by fitting the change in contact area as a function of applied load and using low energy smooth OTS counter-surface.[32,48]

The friction measurements for the range of sliding velocities were measured using a nano-stepper motor (NewFocus) for slow velocities, V, (40 nm/s to 50 μm/s) and a Servo Motor (Moog Animatics SM) with different pitch sizes for faster velocities (4 μm/s to 0.7 m/s). A normal load of 5 mN was used for each experimental trial; where the normal indenting displacement required to achieve 5 mN for each lens was independently verified and applied for each experiment. The shear force was measured using a double-cantilever spring on which a PDMS lens was attached (Figure S3). The cantilever deflection, L, and contact area, A, were measured in each frame of the high-speed video (60 to 30,000 frames per second) recorded using a Photron FASTCAM SA-04 mounted to an Olympus microscope. The cantilever deflection was measured by tracking sharp detectable edges in the video using Pro-analyst (Xcitex) software and the contact area was measured by using an edge detection script in MATLAB (Mathworks). The frictional shear force, F, was calculated by multiplying the deflection by the spring constant, k: $F = kL$. The frictional shear stress, σ_s, was calculated by normalizing the frictional shear force and contact area per fame: $\sigma_s = F/A$. The spring calibration curve and spring constant are shown in Figure S4 is calculated from three repeats] The OTS surfaces were characterized using stylus profilometer and AFM. Data was stitched together via averaging in the region of shared wavenumber q between the stylus profilometer and AFM techniques.[34]

Author Contributions

SD, AD and TDBJ conceptualized and designed the initial experiments. AD supervised, acquired financial support, and administered the project. SD performed the experiments and formal analysis. AG characterized the surface roughness. DM was responsible for the software, methodology, visualization, and formal analysis. LP assisted with the analysis and interpretation of the friction model. DM drafted the initial manuscript, while all the authors contributed to writing, reviewing, and editing the manuscript.

Conflicts of interest

There are no conflicts to declare.

Acknowledgements

We thank Edward Laughlin, the machinist at the University of Akron, for building the in-house friction setup. We thank Prof. BNJ Persson for useful discussions. A.D. acknowledges funding from the NSF (DMR-1610483). TDBJ acknowledges support from the NSF (CMMI-1727378). We thank Anvay Patil, Nathaniel Orndorf and Jiansheng Feng from University of Akron for help in surface roughness characterization of OTS surface.

Notes and references

1 G. Heinrich, M. Klüppel, Wear, 2008, 265, 7-8, 1052-1060.

2 M. Ayyildiz, M. Scaraggi, O. Sirin, C. Basdogan, B. N. Persson, Proc. Natl. Acad. Sci., 2018, 115, 50, 12668-12673.

3 P. Glick, S. A. Suresh., D. Ruffatto, M. Cutkosky, M. T. Tolley, A. Parness, IEEE Robotics and Automation Letters, 2018, 3, 2, 903-910.

4 M. Urbakh, J. Klafter, D. Gourdon, J. Israelachvili, Nature, 2004,430, 525–528.

5 N. Gravish, M. Wilkinson, S. Sponberg, A. Parness, N. Esparza, D. Soto, T. Yamaguchi, M. Broide, M. Cutkosky, C. Creton, K. Autumn, J. R. Soc. Interface, DOI: 10.1098/rsif.2009.0133.

6 N. Gent, J. D. Walter, Pneumatic Tire, https://ideaexchange.uakron.edu/mechanical_ideas/854, accessed: 1, 2022.

7 K. A. Grosch, Proc. R. Soc. Lond. A, 1963, 274, 21.

8 S. P. Arnold, A. D. Roberts, and A. D. Taylor, J. Nat. Rubb. Res., 1987, 2, 1.

9 A. D. Roberts, Rubber Chemistry and Technology, DOI: 10.5254/1.3538633.

10 Schallamach, Wear, 1971, 17, 301.

11 M. Barquins, A. D. Roberts, J. Phys. D: Appl. Phys., 1986, 19, 547-563.

12 M. Barquins, Materials Science and Engineering, 1985, 73, 45-63.

13 K. Viswanathan, A. Mahato, and S. Chandrasekar, Phys. Rev. E, 2015, 91, 012408.

14 K. Viswanathan, N. K. Sundaram, S. Chandrasekar, Soft Matter, 2016, 12, 5265-5275.

15 K. Viswanathan, N. K. Sundaram, S. Chandrasekar, Soft Matter, 2016, 12, 9185.

16 K. Viswanathan, N. K. Sundaram, Wear, 2017, 376-377, 1271-1278.

17 A. Schallamach, Proc. Phys. Soc. Sect. B, 1953, 66, 386.

18 Y. B. Chernyak and A. I. Leonov, Wear, 1986, 108, 2, 105-138.

19 K. Vorvolakos and M. K. Chaudhury, Langmuir, 2003, 19, 6778.

20 L. Pastewka, M. Robbins, Proc. Natl. Acad. Sci., 2014, 111, 2398.

21 M. Müser, Tribol. Int., 2016, 100, 41.

22 B. N. J. Persson, J. Chem. Phys., 2001, 115, 3840.

23 B. N. J. Persson, O. Albohr, U. Tartaglino, A. I. Volokitin, and E. Tosatti, J. Phys. Condens. Matter, 2005, 17, R1.

24 B. N. J. Persson, J. Phys. Condens. Matter, 2008, 20, 312001.

25 B. N. J Persson, Surface Science, 1998, 401, 3, 445-454.

26 M. Scaraggi, B. N. J. Persson, , J. Phys.: Condens. Matter, 2015, 27, 105102.

27 B. Lorenz, Y. R. Oh, S. K. Nam, S. H. Jeon, and B. N. J. Persson, J. Chem. Phys., 2015, 142, 194701.

28 A. Tiwari, N. Miyashita, N. Espallargas, and B. N. J. Persson, J. Chem. Phys., 2018, 148, 224701.

29 Genovese, F. Farroni, A. Papangelo, and M. Ciavarella, Lubricants, DOI: 10.3390/lubricants7100085.

30 M. Klüppel, G. Heinrich, Rubber Chemistry and Technology, 2000,73, 4, 578–606.

31 A. N. Gent, Langmuir, 1996, 12, 19, 4492-4496.

32 A. P. Defante, T. N. Burai, M. L. Becker, A. Dhinojwala, Langmuir, 2015, 31(8), 2398-2406.

33 T. D. B. Jacobs, T. Junge, and L. Pastewka, Surf. Topogr. Metrol. Prop., 2017, 5, 013001.

34 S. Dalvi, A. Gujrati, S. R. Khanal, L. Pastewka, A. Dhinojwala, and T. D. B. Jacobs, Proc. Natl. Acad. Sci., 2019, 116, 25484.

35 A. Lorenz, B. A. Krick, N. Mulakaluri, M. Smolyakova, S. Dieluweit, W. G. Sawyer, and B. N. J. Persson, J. Phys. Condens. Matter, 2013, 25, 225004.

36 A.Gujrati, A. Sanner, S. R. Khanal, N. Moldovan, H. Zeng, L. Pastewka, T. D. B. Jacobs, Surf. Topogr.: Metrol. Prop., 2021, 9, 014003.

37 R. Aghababaei, D. H. Warner, J.-F. Molinari, Nature Communications, 2016, 7, 11816.

38 Maugis, Journal of Colloid and Interface Science, 1992, 150, 1, 243-269.

39 K. C. Ludema, D. Tabor, Wear, 1966, 9, 5, 329-348.

40 M. Müser, B.N.J Persson, EPL, 2022, 137, 36004.

41 B.N.J Persson, E. Brener, Phys. Rev. E, 2005, 71, 036123.

42 B. N. J. Persson, Eur. Phys. J. E, 2002, 8, 385–401.

43 O. Kulikov, K. Hornung, J. Non-Newtonian Fluid Mech., 2004, 124, 103-114.

44 V. Vaenkatesan, Z. Li, W. P. Vellinga, W. H. de Jeu, Polymer, 47, 2006, 8317–8325.

45 S. R. Wasserman, Y. T. Tao, G. M. Whitesides, Langmuir, 1989, 5(4), 1074-1087.

46 S. N. Dalvi, Understanding Contact Mechanics and Friction on Rough Surfaces, 2020, (Doctoral dissertation, University of Akron).

47 A. Kurian, S. Prasad, A. Dhinojwala, Macromolecules, 2010, 43(5), 2438-2443.

48 K. L. Johnson, K. Kendall, A. Roberts, Proc. R. Soc. Lond. A., 1971, 324(1558), 301-313.